Solving the Kadanoff-Baym Equations for Inhomogeneous Systems: Application to Atoms and Molecules

Nils Erik Dahlen and Robert van Leeuwen

Theoretical Chemistry, Zernike Institute for Advanced Materials, University of Groningen, Nijenborgh 4, 9747 AG Groningen, The Netherlands

(Received 2 October 2006; published 13 April 2007)

We implement time propagation of the nonequilibrium Green function for atoms and molecules by solving the Kadanoff-Baym equations within a conserving self-energy approximation. We here demonstrate the usefulness of time propagation for calculating spectral functions and for describing the correlated electron dynamics in a nonperturbative electric field. We also demonstrate the use of time propagation as a method for calculating charge-neutral excitation energies, equivalent to highly advanced solutions of the Bethe-Salpeter equation.

DOI: 10.1103/PhysRevLett.98.153004 PACS numbers: 31.25.−v, 31.10.+z

The arrival of molecular electronics has exposed the need for improved methods for first-principles calculations on nonequilibrium quantum systems [1]. The nonequilibrium Green function [2,3] is for several reasons a natural device in such studies. Not only is it relatively simple, being a function of two coordinates, but it contains a wealth of information, including the electron density and current, the total energy, ionization potentials, and excitation energies. Time propagation according to the Kadanoff-Baym equations [3,4] is a direct method for describing the correlated electron dynamics and a method which automatically leads to internally consistent and unambiguous results in agreement with macroscopic conservation laws. In the linear response regime, time propagation within relatively simple self-energy approximations corresponds to solving the Bethe-Salpeter equation with highly advanced kernels [5]. The Green function techniques are also highly interesting as a complementary method to time-dependent density functional theory (TDDFT) [6,7], not only by providing benchmark results for testing new TDDFT functionals, but diagrammatic techniques can also be used to systematically derive improved density functionals [8]. We will in this Letter demonstrate time propagation for inhomogeneous systems, using the beryllium atom and the H_2 molecule as illustrative examples.

The nonequilibrium Green function $G(\mathbf{x}t, \mathbf{x}'t')$ depends on two time variables rather than one, such as the time-dependent many-particle wave function. On the other hand, the fact that it also depends on only two space and spin variables $\mathbf{x} = (\mathbf{r}, \sigma)$ means that it can be used for calculations on systems that are too large for solving the time-dependent Schrödinger equation, such as the homogeneous electron gas [5] or solids [9], or for calculations on molecular conduction. In addition, the Green function provides information about physical properties, such as ionization potentials and spectral functions, that are not given by the many-particle wave function. The Green function techniques also have the advantage over, e.g., TDDFT or density matrix methods based on the Bogoliubov-Born-Green-Kirkwood-Yvon hierarchy [10] that it is easy to find approximations which give observables in agreement with macroscopic conservation laws.

The two time arguments of the Green function are located on a time contour as illustrated in Fig. 1. It solves the equation of motion (we suppress the space and spin variables for notational simplicity)

$$[i\partial_t - h(t)]G(t, t') = \delta(t, t') + \int_C d\bar{t}\Sigma(t, \bar{t})G(\bar{t}, t'), \quad (1)$$

where $h(t)$ is the noninteracting part of the Hamiltonian (which may include an arbitrarily strong time-dependent potential), and the self-energy Σ accounts for the effects of the electron interaction. We use atomic units throughout. The time integral is performed along the contour, and the delta function $\delta(t, t')$ is defined on the contour [11]. We consider only systems initially (at $t = 0$) in the ground state. This is facilitated by describing the system within the finite-temperature formalism [12], letting the time contour start at $t = 0$ and end at the imaginary time $t = -i\beta = -i/(k_B T)$, as illustrated in Fig. 1. This choice of initial conditions means that the first step consists of calculating the Green function for both time arguments on the imagi-

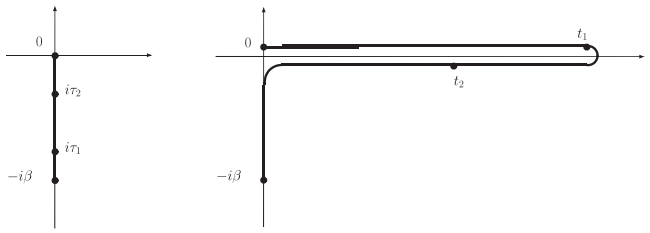

FIG. 1. At $t = 0$, the system is in thermal equilibrium, and the Green function is calculated for imaginary times from 0 to $-i\beta$ (left). Describing the system for $t > 0$ implies calculating $G(t_1, t_2)$ on an extending time contour (right).

nary track. The calculations are carried out in a basis of Hartree-Fock (HF) molecular orbitals, such that $G(\mathbf{x}t, \mathbf{x}'t') = \sum_{i,j}\phi_i(\mathbf{x})G_{ij}(t,t')\phi_j^*(\mathbf{x}')$. The Green function is consequently represented as a time-dependent matrix, and the equations of motion reduce to a set of coupled matrix equations. The HF orbitals $\phi_i(\mathbf{x})$ are themselves given by linear combinations of Slater functions centered on the nuclei of the molecule.

We have solved the Kadanoff-Baym equations within the second-order self-energy approximation, illustrated in Fig. 2. This is a conserving approximation [13,14], which is essential for obtaining results in agreement with macroscopic conservation laws. This is easily verified numerically, for instance, by checking that the total energy remains constant when the Hamiltonian is time-independent. For a given $G(t,t')$ matrix, the self-energy matrix (for a spin-unpolarized system) is given by $\Sigma(t,t') = \delta(t,t')\Sigma^{\mathrm{HF}}(t) + \Sigma^{(2)}(t,t')$, where

$$\Sigma_{ij}^{(2)}(t,t') = \sum_{klmnpq} G_{kl}(t,t')G_{mn}(t,t')G_{pq}(t',t) \times v_{iqmk}(2v_{lnpj} - v_{nlpj}), \tag{2}$$

and $\Sigma_{ij}^{\mathrm{HF}}(t) = -i\sum_{kl}G_{kl}(t,t^+)(2v_{ilkj} - v_{iljk})$ is the HF self-energy. The two-electron integrals are defined by

$$v_{ijkl} = \iint d\mathbf{x}d\mathbf{x}'\phi_i^*(\mathbf{x})\phi_j^*(\mathbf{x}')v(\mathbf{r}-\mathbf{r}')\phi_k(\mathbf{x}')\phi_l(\mathbf{x}). \tag{3}$$

As the initial Hamiltonian is time-independent, the Green function on the imaginary track of the contour depends only on the difference between the two imaginary time coordinates. Solving for $G^M(i\tau - i\tau') \equiv G(-i\tau, -i\tau')$ (we use τ to denote time arguments on the imaginary axis) is then equivalent to solving the ordinary Dyson equation within the finite-temperature formalism [15]. Note that the definition of G^M in Ref. [16] differs from the one used here by a prefactor i. Since the self-energy is a functional of the Green function, the Dyson equation should be solved to self-consistency.

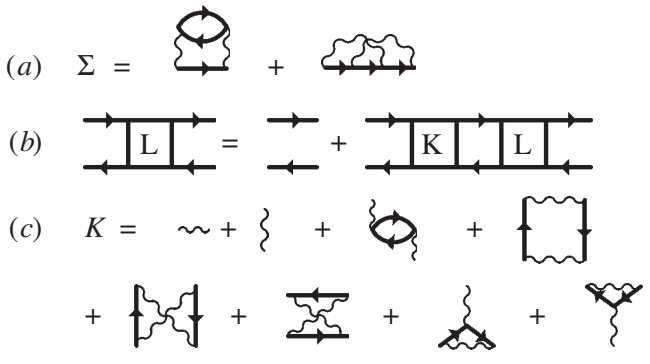

FIG. 2. (a) The correlation part of the second-order self-energy, (b) a diagrammatic representation of the Bethe-Salpeter equation, and (c) the corresponding Bethe-Salpeter kernel. The Green function lines represent self-consistent, full Green functions.

Once the equilibrium Green function has been calculated, it can be propagated according to the Kadanoff-Baym equations [3]. Time propagation means that the contour which initially goes along the imaginary axis is extended along the real axis (see Fig. 1). The Green functions with both arguments on the real time axis are denoted by the functions $G_{ij}^{>}(t,t') = -i\langle\hat{c}_i(t)\hat{c}_j^\dagger(t')\rangle$ (if t is later on the contour than t') and $G_{ij}^{<}(t,t') = i\langle\hat{c}_j^\dagger(t')\hat{c}_i(t)\rangle$ (if t' is later than t), with the symmetry $[G_{ij}^{\lessgtr}(t,t')]^* = -G_{ji}^{\lessgtr}(t',t)$ and the boundary condition $G_{ij}^{>}(t,t) - G_{ij}^{<}(t,t) = -i\delta_{ij}$. We also need to calculate the functions $G^{\rceil}(t,i\tau)$ and $G^{\lceil}(i\tau,t)$ with one real and one imaginary time argument. The implementation of the propagation is similar to the scheme described by Köhler *et al.* in Ref. [17], with one important difference being that we are dealing here with an inhomogeneous system; i.e., the Green function, self-energy, and $h(t)$ are time-dependent matrices rather than vectors.

Another important difference with the propagation scheme described in Ref. [17] is the initial correlations. In our case, they are given by the equilibrium Green function according to $G^{<}(0,0) = G^M(0^-)$ and $G^{\rceil}(0,-i\tau) = G^M(-i\tau)$. Because of the antiperiodicity $G^M(i\tau + i\beta) = -G^M(i\tau)$, the resulting nonequilibrium Green function will automatically satisfy the Kubo-Martin-Schwinger boundary condition $G(0,t) = -G(-i\beta,t)$. The time stepping follows the four coupled Kadanoff-Baym equations

$$\begin{aligned}[i\partial_t - h(t)]G^{>}(t,t') &= I_1^{>}(t,t'),\\ [i\partial_t - h(t)]G^{\rceil}(t,i\tau) &= I^{\rceil}(t,i\tau)\end{aligned} \tag{4}$$

and the two corresponding adjoint equations [16]. The collision integrals are

$$I_1^{>}(t,t') = \int_0^t d\bar{t}\Sigma^R(t,\bar{t})G^{>}(\bar{t},t') + \int_0^{t'} d\bar{t}\Sigma^{>}(t,\bar{t})G^A(\bar{t},t') + \frac{1}{i}\int_0^\beta d\bar{\tau}\Sigma^{\rceil}(t,-i\bar{\tau})G^{\lceil}(-i\bar{\tau},t'), \tag{5}$$

$$I^{\rceil}(t,i\tau) = \int_0^t d\bar{t}\Sigma^R(t,\bar{t})G^{\rceil}(\bar{t},i\tau) + \frac{1}{i}\times\int_0^\beta d\bar{\tau}\Sigma^{\rceil}(t,-i\bar{\tau})G^M(i\bar{\tau}-i\tau). \tag{6}$$

The retarded and advanced functions $G^{R/A}$ and $\Sigma^{R/A}$ are defined according to $F^{R/A}(t,t') = \delta(t-t')F^\delta(t) \pm \theta(\pm t \mp t')[F^{>}(t,t') - F^{<}(t,t')]$, where only the self-energy has a singular part (the HF self-energy). The last terms in each of Eqs. (5) and (6) account for the initial correlations of the system and do not vanish when $t, t' \to 0$.

We have been able to propagate the Green function for a number of closed-shell atoms and small diatomic molecules, where one can aim at quantitative agreement with experimental results. The kind of calculations presented in

this Letter typically take 48 hours. The basis set must be large enough to describe the essential details of the electron dynamics. The most important limiting factor is the energy level structure of the systems; for heavier atoms, the large eigenenergies of the core levels lead to rapid oscillations in the Green function, and one consequently needs to propagate using time steps much smaller than the time scale of the interesting physical phenomena dominated by the valence electrons. We have in these calculations used 28 basis functions for beryllium and 25 functions for H_2, with orbital energies lower than 5 Hartree. We include a time-dependent electric field in the direction of the molecular axis, so that the system preserves a cylindrical symmetry. Generalizing this scheme to systems of lower symmetry does not lead to complications other than increasing the size of the calculations. Since the systems considered here have only discrete energy levels, we do not observe strong damping effects such as what is observed in systems with a continuous spectrum [17,18].

Figure 3 shows the imaginary part of $\mathrm{Tr}\{G^<(t_1, t_2)\}$, calculated for an H_2 molecule in equilibrium and in the presence of a constant electric field $E(t) = \theta(t)E_0$ directed along the molecular axis. In both cases, the trace of $G^<$ along the time diagonal is constant and equal to the particle number. In the ground state (shown to the left), the Green function depends only on the difference $t_1 - t_2$, and the oscillations perpendicular to the time diagonal are given by the ionization potentials of the molecule. The right figure illustrates how the electric field ($E_0 = 0.14$ a.u.) changes the spectral properties of the molecule. In addition to the expected narrowing of the ridge along the time diagonal, the oscillations along the $t_1 - t_2$ direction are damped. In the upper figures, we show $\mathrm{Im}\,\mathrm{Tr}\{G^<(t_1, t_2)\}$ for a fixed $T = (t_1 + t_2)/2 = 20$ a.u., compared with the same function calculated from time-dependent HF (TDHF). The ground-state HF Green function has the form $\mathrm{Tr}\{G^<_{\mathrm{HF}}(t_1, t_2)\} = i\sum_i n_i e^{-i\epsilon_i(t_1 - t_2)}$, and for the H_2 molecule we therefore have $\mathrm{Im}\,\mathrm{Tr}\{G^<_{\mathrm{HF}}(T + t/2, T - t/2)\} = 2\cos(\epsilon_1 t)$. The correlated Green function has a sharper peak at $t = 0$, and, while it is periodic in the relative time coordinate, it is characteristic of a correlated spectral function that it cannot be fitted to a cosine function at small t [10]. With an added electric field, the energy fed into the system leads to a narrowing of the spectral function peak.

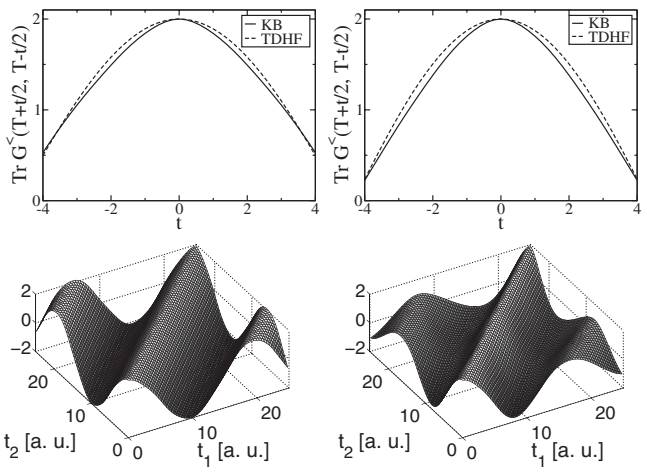

FIG. 3. The lower figures show the trace of the imaginary part of $G^<(t_1, t_2)$ for an H_2 molecule in its ground state (left) and in an applied electric field (right). The Green function in equilibrium depends only on $t_1 - t_2$. The upper figures show the same quantity for a fixed value of $T = (t_1 + t_2)/2$, compared with the same function obtained from TDHF.

Time propagation is also useful as a direct method for calculating response functions and excitation energies [5]. The excitation energies of the system can be obtained from the poles of the density response function $\chi(\omega)$, defined by $\delta n(\omega) = \chi^R(\omega)\delta v(\omega)$. Perturbing the system with a "kick" of the form $\delta v(t) = V\delta(t)$ excites all states compatible with the symmetry of the perturbing potential V. For a kick in the form of an electric field along the molecular axis, the induced dipole moment is given by $d(t) = E_0 \int d\mathbf{r}d\mathbf{r}' z\chi^R(\mathbf{r}, \mathbf{r}'; t)z'$. The imaginary part of the Fourier transformed dipole moment then has peaks at the poles of $\chi^R(\omega)$, corresponding to the excitation energies of the system. Time propagation is in this way an interesting and far more direct alternative to calculating the response function from $\chi(1, 2) = L(1, 2; 1, 2)$, where the particle-hole propagator L is found by solving the Bethe-Salpeter equation [13,14] $L = L_0 + L_0KL$, as illustrated diagrammatically in Fig. 2. The self-energy approximation used in this Letter would correspond to the kernel $K = \delta\Sigma/\delta G$ shown in Fig. 2, where it should be noted that the Green functions are the full Green functions of the interacting system. In Fig. 4, we have plotted the imaginary part of the polarizability, defined according to $\alpha_T(\omega) = -1/E_0 \int_0^T dt e^{i\omega t} d(t)$, of a beryllium atom for various durations T of the time propagation. The polarizability develops a distinct peak at the $^1S \rightarrow {}^1P$ transition energy $\omega = 0.189$ a.u. (compared to the TDHF value of 0.178

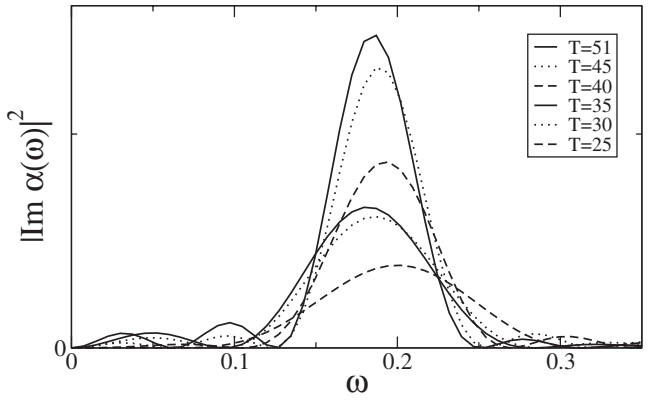

FIG. 4. The imaginary part of the polarizability $\alpha(\omega)$ of a beryllium atom calculated from the Green function propagated up to a time T.

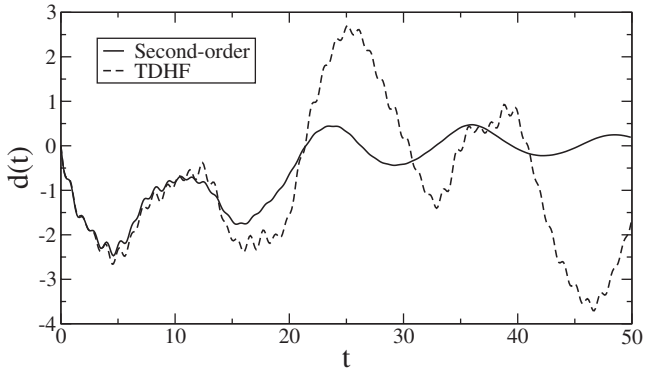

FIG. 5. The time-dependent dipole moment of a Be atom, calculated within the HF and the second-order approximation.

calculated within the same basis, and the experimental value of 0.194 [19]), which becomes increasingly sharp as the propagation time is extended. As the system consists only of discrete energy levels, the damping of the time-dependent dipole moment $d(t)$ as a function of time is not significant in the relatively short duration of the time propagation. The position of the excitation energy peak in Fig. 4 therefore converges slowly, but extrapolation schemes nevertheless give the position of the peak very accurately.

In Fig. 5, we have plotted the time-dependent dipole moment of the beryllium atom, this time with a nonperturbative kick at $E_0 = 1.0$ a.u. In this case, we see a clear difference between the uncorrelated Hartree-Fock result and the dipole moment calculated from the Kadanoff-Baym equations. The difference between the correlated and the uncorrelated results becomes more apparent with time, due to the nonlinear effects entering via the self-energy. Since we have now excited all unoccupied states, we can expect some damping in the time-dependent dipole moment, but the damping is much more pronounced in the correlated calculation.

In conclusion, we have demonstrated that time propagation of the nonequilibrium Green function can be used as a practical method for calculating nonequilibrium and equilibrium properties of atoms and molecules (e.g., for atoms in strong laser fields). For these small systems, the second-order approximation is clearly well-suited. For extended systems, such as molecular chains, it becomes essential to cut down the long range of the Coulomb interaction. This is done effectively within the GW approximation [20,21] (known as the shielded potential approximation in Refs. [13,14]), where the self-energy is given as a product of the Green function G and the dynamically screened interaction W and which we have currently implemented for the ground state [22]. For calculations involving heavier atoms, it will be necessary to use pseudopotentials in order to avoid the very short time steps necessary to account for the core levels. For larger molecules or solids, the calculations are certainly feasible in the framework of model Hamiltonians that include electron interaction. Green function calculations are therefore highly important (i) for providing benchmark results for simpler methods, (ii) for investigating the role of electron correlation, and (iii) as an alternative to solving the Bethe-Salpeter equation with highly sophisticated kernels.

[1] Y. Xue, S. Datta, and M. A. Ratner, Chem. Phys. **281**, 151 (2002).
[2] L. V. Keldysh, Zh. Eksp. Teor. Fiz. **47**, 1515 (1964) [Sov. Phys. JETP **20**, 1018 (1965)].
[3] L. P. Kadanoff and G. Baym, *Quantum Statistical Mechanics* (Benjamin, New York, 1962).
[4] W. Schäfer, J. Opt. Soc. Am. B **13**, 1291 (1996); M. Bonitz, D. Kremp, D. C. Scott, R. Binder, W. K. Kraeft, and H. S. Köhler, J. Phys. Condens. Matter **8**, 6057 (1996); R. Binder, H. S. Köhler, M. Bonitz, and N. Kwong, Phys. Rev. B **55**, 5110 (1997).
[5] N.-H. Kwong and M. Bonitz, Phys. Rev. Lett. **84**, 1768 (2000).
[6] E. Runge and E. K. U. Gross, Phys. Rev. Lett. **52**, 997 (1984).
[7] M. A. L. Marques, C. A. Ullrich, F. Nogueira, A. Rubio, K. Burke, and E. K. U. Gross, *Time-Dependent Density Functional Theory* (Springer, Berlin, 2006).
[8] R. van Leeuwen, Phys. Rev. Lett. **76**, 3610 (1996).
[9] H. Haug and A.-P. Jauho, *Quantum Kinetics in Transport and Optics of Semiconductors* (Springer, Berlin, 1998); N.-H. Kwong, M. Bonitz, R. Binder, and H. S. Köhler, Phys. Status Solidi B **206**, 197 (1998).
[10] M. Bonitz, *Quantum Kinetic Theory* (Teubner, Stuttgart, 1998).
[11] P. Danielewicz, Ann. Phys. (N.Y.) **152**, 239 (1984).
[12] We here consider only finite systems, for which the finite-temperature formalism is used as a formal device for imposing boundary conditions on the Green function but is only meaningful in the $T \rightarrow 0$ limit.
[13] G. Baym and L. P. Kadanoff, Phys. Rev. **124**, 287 (1961).
[14] G. Baym, Phys. Rev. **127**, 1391 (1962).
[15] N. E. Dahlen and R. van Leeuwen, J. Chem. Phys. **122**, 164102 (2005).
[16] N. E. Dahlen, R. van Leeuwen, and A. Stan, J. Phys.: Conf. Ser. **35**, 340 (2006).
[17] H. S. Köhler, N. H. Kwong, and H. A. Yousif, Comput. Phys. Commun. **123**, 123 (1999).
[18] D. Semkat, D. Kremp, and M. Bonitz, Phys. Rev. E **59**, 1557 (1999).
[19] A. Kramida and W. C. Martin, J. Phys. Chem. Ref. Data **26**, 1185 (1997).
[20] L. Hedin, Phys. Rev. **139**, A796 (1965).
[21] F. Aryasetiawan and O. Gunnarsson, Rep. Prog. Phys. **61**, 237 (1998).
[22] A. Stan, N. E. Dahlen, and R. van Leeuwen, Europhys. Lett. **76**, 298 (2006).